3

Attempted ROMP of cage alkenes

The results of the ROMP of a variety of cage alkenes with the well-defined ruthenium carbene catalysts **55** (Grubbs-I) and **56** (Grubbs-II) are described in this chapter. These catalysts were selected because of their commercial availability, stability towards polar functionalities, and because they have been shown to affect the ROMP of low strain monomers such as cyclopentene, cycloheptene and substituted cyclopentenes.[95,219]

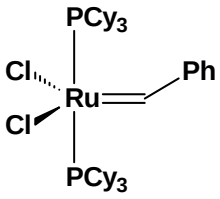

55

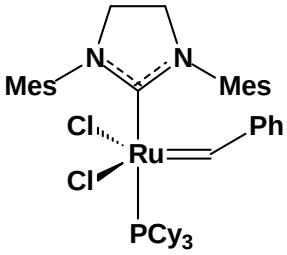

56

3.1. ROMP of cage alkenes

In a typical experiment the monomer was dissolved in dry THF in a small vial. A magnetic stirrer was added, followed by a mass of catalyst that would give a monomer-to-catalyst ratio of approximately 50:1. This is a high catalyst loading. Ritter *et. al*[88] suggested using 1,5-cyclooctadiene with a 0.1 mol% catalyst loading as a benchmark system when testing new catalysts for ROMP reactivity. However, in this study different monomers were used and the catalysts were kept the same. In such cases monomer-to-catalyst ratio of up to 20:1 has been reported.[220] The monomer-to-catalyst ratio selected in this study is a compromise since the purpose of the study was to determine whether or not it is possible to polymerise the selected cage alkenes and not to determine the optimal conditions for such polymerisation reactions. The results of ROMP reactions with a number of cage monomers are summarised in **Table 3.1**. Experimental details are reported in **Table 4.1** (➡ p. 119). The results in **Table 3.1** show that ROMP of the cage alkenes initially selected in this study did not meet with much success. Only the cage monomers **3** and **127** showed some reactivity. The results seem to indicate that endocyclic monomers with a tetracycloundecane (TCU) framework are not reactive towards ROMP. In the successful experiments Grubbs-II proved the superior catalyst. For example, Grubbs-II yielded 15% polymer on reaction with **127** compared to the 7% yield obtained when using Grubbs-I.

Table 3.1: ROMP of cage monomers with Grubbs-I and Grubbs-II

Monomer	Solvent	Catalyst	Monomer to Catalyst ratio	Time (h)	t (^oC)	Yield
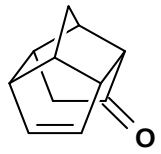 **1**	THF	Gr^I	50: 1	24	25	–
	THF	Gr^{II}	50: 1	24	25	–
	THF	Gr^{II}	50: 1	24	66	–
	THF	Gr^{II}	50: 1	24	66	–
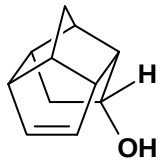 **118**	THF	Gr^I	50: 1	24	25	–
	THF	Gr^{II}	46: 1	24	25	–
	THF	Gr^{II}	50: 1	20	25	–
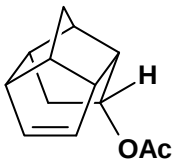 **121**	THF	Gr^I	45: 1	24	25	–
	THF	Gr^{II}	49: 1	24	25	–
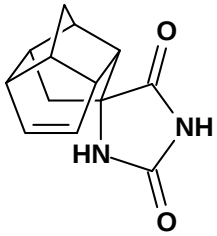 **156**[32]	$CHCl_3$	Gr^I	42: 1	24	25^oC	–
	$CHCl_3$	Gr^{II}	36: 1	24	25^oC	–
	$CHCl_3$	Gr^{II}	50: 1	5	61^oC	–
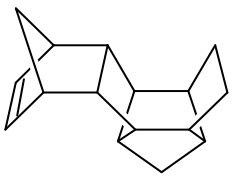 **127**	THF	Gr^I	50: 1	24	25	7%
	THF	Gr^{II}	42: 1	24	25	15%
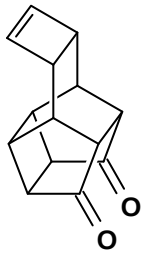 **3**	THF	Gr^I	50: 1	20	45	21%
	THF	Gr^{II}	50: 1	20	45	45%
	THF	Gr^{II}	50: 1	20	45	52%
	THF	Gr^{II}	1000: 1	48	25	42%

3.2. NMR investigation of the ROMP reaction

The ROMP reactions of the cage monomers in **Table 3.1** were investigated further with NMR spectroscopy. The experimental details used during the NMR experiments are provided in **Table 4.2** (➡ p. 121). NMR spectra collected for **3** and Grubbs-II are shown in **Figure 3.1**. The conversion of **3** to polymer was determined from the ratio of the integral of the olefinic protons at δ_H 6.27 and the TMS signal at δ_H 0.00. Initially, the ratio of the integral of the olefinic protons of **3** and the chloroform signal was used until it was realised that the signal of a decomposition product of Grubbs-II overlaps with the chloroform signal. The polymer produced from **3** precipitated in the tube during the course of the NMR experiment. The precipitate was sufficiently insoluble that no signals of the product could be detected in the NMR spectra.

The possible ROMP of **1** was investigated next. The progress of the reaction was determined from the ratio of the integral of the olefinic protons at δ_H 6.04 and the TMS signal at δ_H 0.00 (**Figure 3.2**). No precipitate formed during the NMR experiment and no polymer product could be detected in the NMR spectra. The experiment was repeated in benzene to eliminate the possibility of peak overlap. In another NMR experiment the data range was extended to 30 ppm to make sure that no new carbene signals remain undetected. The interpreted NMR data for the ROMP of **3** and the attempted ROMP of **1** are compared in **Figure 3.3**. The graphs show that the cage monomer **1** is not reactive towards ROMP. It can also be deduced that coordination between **1** and Grubbs-II is unlikely since a 1:1 combination would result in a 2% decrease in the monomer concentration.

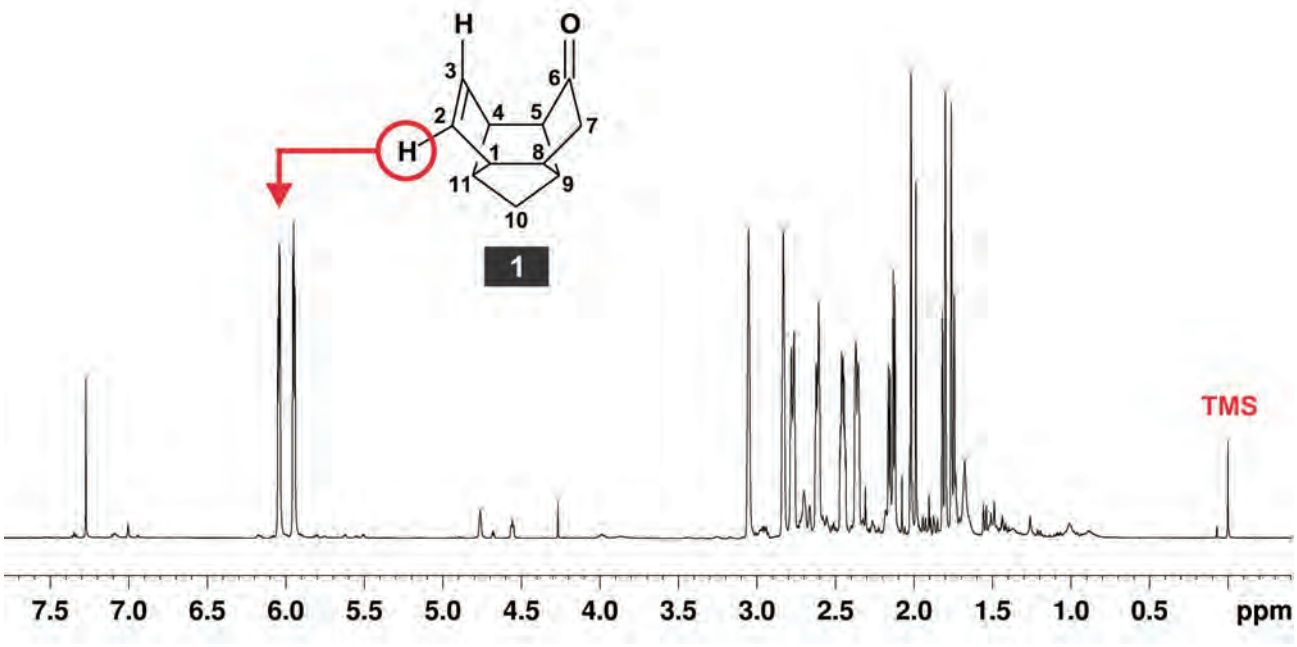

Figure 3.2: Monitoring of the possible ROMP of **1** in the presence of Grubbs-II.

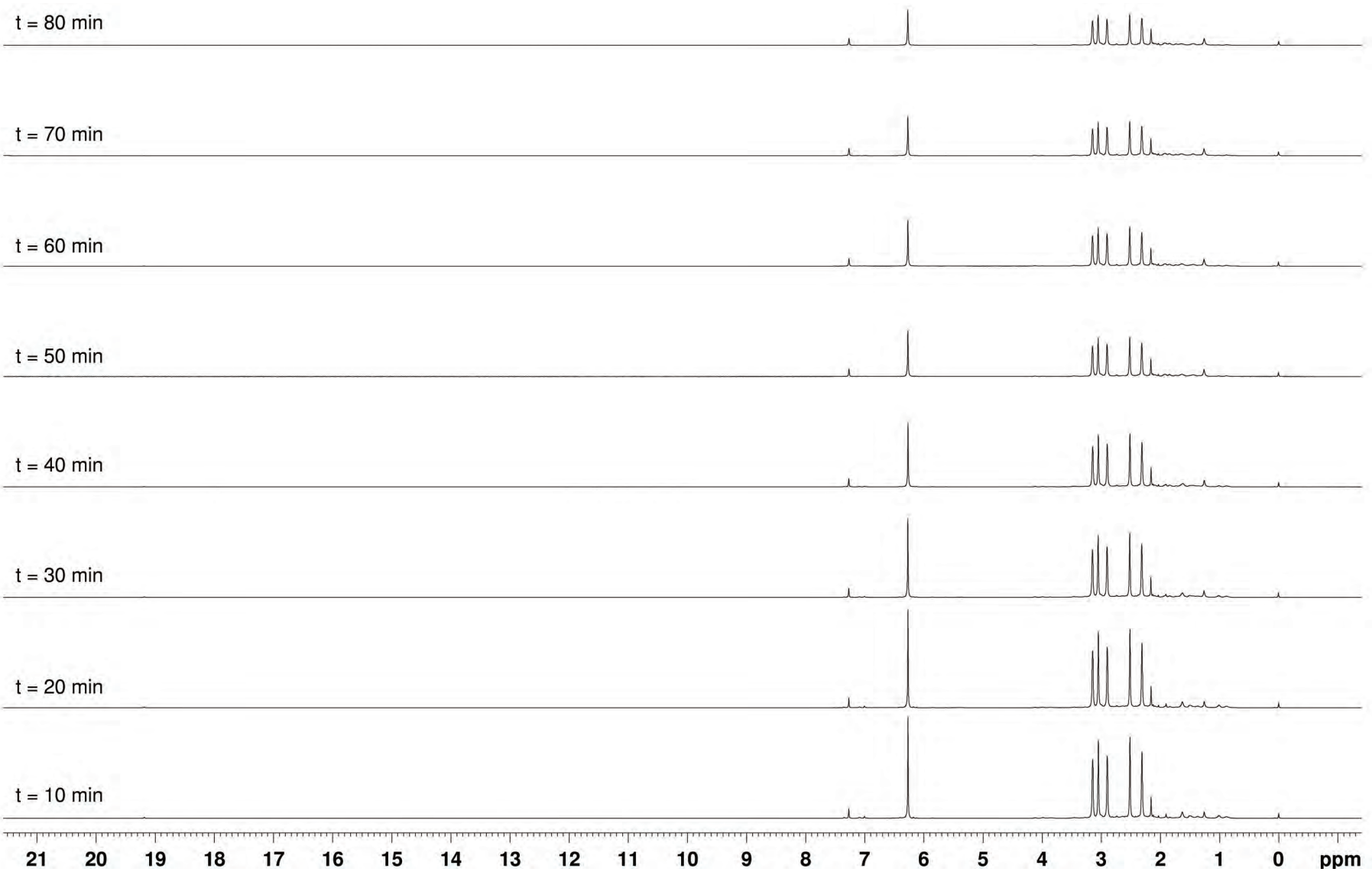

Figure 3.1: Monitoring of the ROMP of **3** in the presence of Grubbs-II.

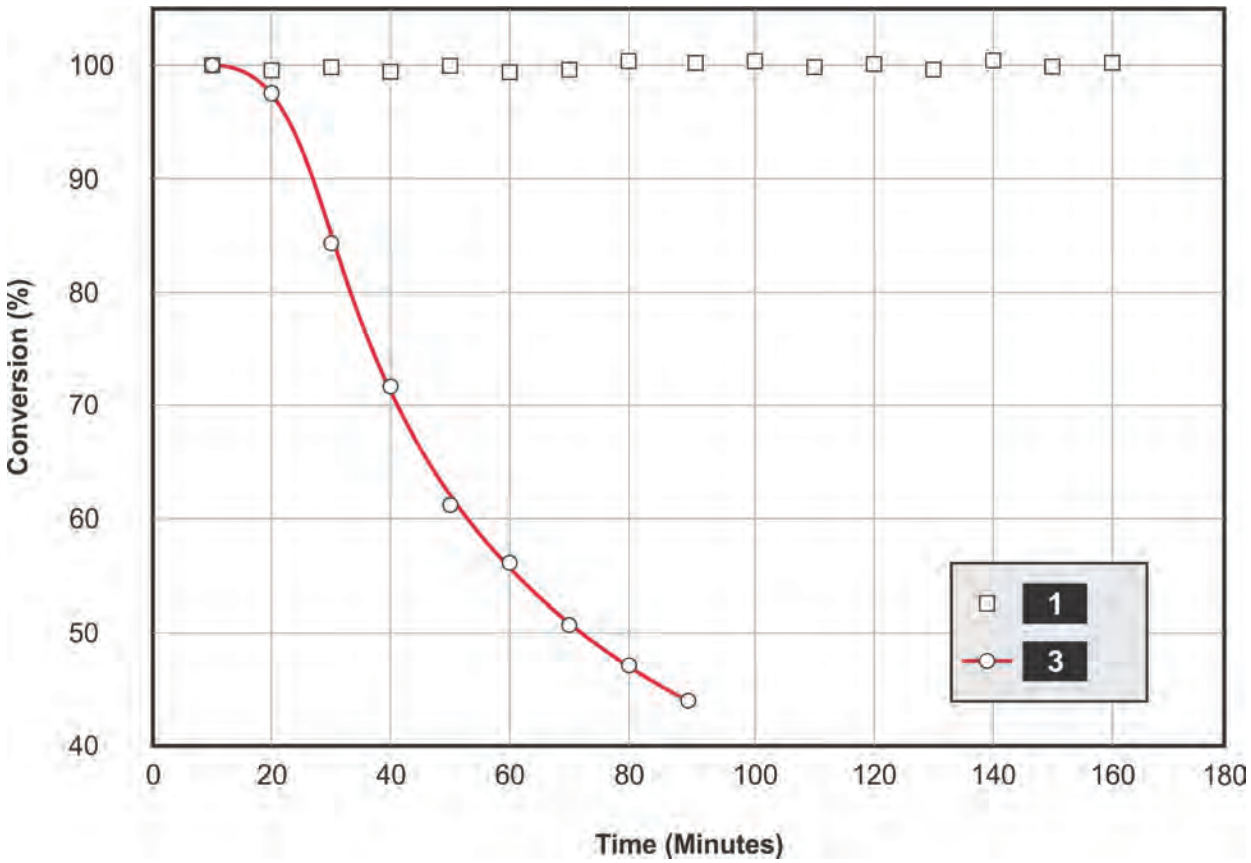

Figure 3.3: Progress of the possible ROMP reactions of **1** and **3**.

An additional experiment was performed to verify that no coordination took place between **1** and Grubbs-II. An equimolar mixture of **1** and Grubbs-II was stirred in chloroform at 40^{o}C for 12 hours. After this time an excess amount of styrene (capping reagent) was added. Analysis of the reaction mixture revealed unreacted styrene and stilbene (the metathesis product of styrene) at *m/z* 180. The product **157** was expected from a 1: 1 combination between **1** and Grubbs-II. The presence of such a compound could not be detected at *m/z* 340.

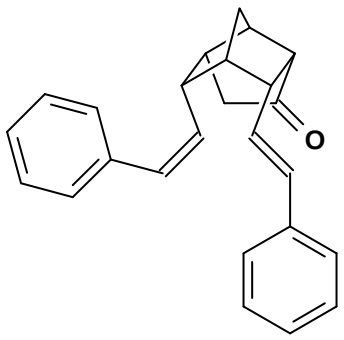

157

3.3. Rationalisation of the experimental results

In this section some attempts at rationalising the experimental results are presented.

3.3.1. Ring strain

Strain exists in a molecule when bonds are forced to make abnormal angles.[221] Angle distortions in molecules manifest as higher potential energy than would be the case in their absence. One of the causes of strain in molecules is the presence of one or more small rings in the carbon framework. Small rings have bond angles that deviate from those formed by normal overlap of orbitals.[222] The ring strain energy (RSE) is a measure of the amount of ring strain present in a molecule. It is defined as the increase in energy created upon ring closure of an acyclic molecule.[223] Strain energy can be estimated by subtracting the energy of a "normal" unstrained reference compound from the energy of a strained compound. The data required for the estimation can be obtained from experiments or theoretical models. Since the advent of molecular modelling, computer-generated data have been used extensively to estimate strain energies.

It was pointed out earlier that ring strain is an important driving force for ROMP (➡ p. 13). Values used in the calculations of RSEs in this study were calculated with DFT/B3LYP/6-31G** on Spartan'08. Prior to employment, the reliability of this computational method was tested. A comparison was made between the calculated values and experimental RSEs. The homodesmotic[b] reaction that was used in the calculation of the RSEs is shown in **Scheme 3.1**.

Scheme 3.1: Homodesmotic reaction used to calculate RSEs of cyclic alkenes.

Figure 3.4 shows the correlation between the data obtained in this study and experimental results published in the literature.[221] The RSEs calculated with DFT/B3LYP/6-31G** correlate well with the experimental values and give significantly better results than the semi-empirical method shown for comparison. The latter method underestimates the RSEs of small rings and overestimates the RSEs of larger rings. The applicability of the computational method for estimation of the RSEs of aliphatic polycyclic compounds, including cage compounds, was determined next. Homodesmotic reactions[224-225] were defined for this purpose.

[b] The term "homodesmic" has also been used. See for example Bachrach, S.M., *J. Chem. Educ.*, 1990, **67**, 907.

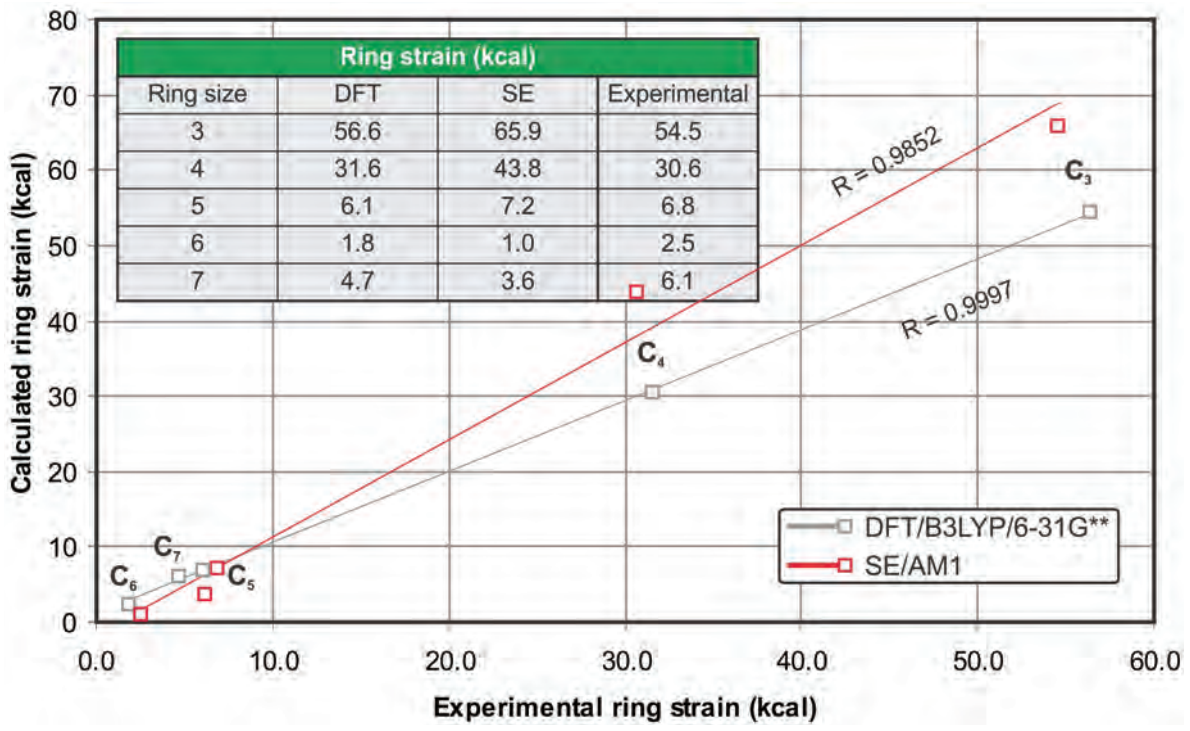

Figure 3.4: Correlation between calculated and experimental RSEs.

Scheme 3.2 shows the homodesmotic reaction used to calculate the RSE of norbornene (**158**).[223]

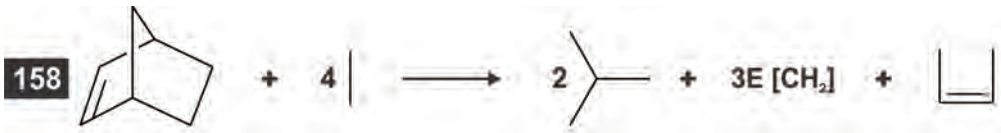

Scheme 3.2: Homodesmotic reaction used to calculate RSE of norbornene.

In this equation, E[CH_2] is the difference in energy between pentane and butane. The RSE is found by subtracting the sums of the energies of the products from the sum of the energies of the reagents. Some results of these calculations are shown in **Table 3.2**. The good correlation obtained for both monocyclic and polycyclic compounds provided support for continued use of this method in the study.

3.3.1.1. ROMP and RSEs of cage alkenes

Norbornene and substituted norbornenes are the most important monomers for ROMP.[4] The RSE of norbornene is estimated to be between 19.2 and 27.2 kcal·mol^{-1} (**Table 3.2**). Clearly, ROMP of norbornene does not release all the RSE contained within the compound. It is therefore an oversimplification to state that norbornene is a good monomer for ROMP because of its high RSE.

Table 3.2: Calculated and experimental RSEs of norbornene and cage compounds

Compound	Homodesmotic reaction	RSE (kcal·mol^{-1})	
		This work	Literature
158	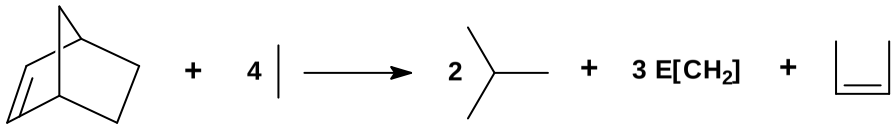	21.7	19.2[221], 21.6[223], 22.8[226], 27.2[227]
25	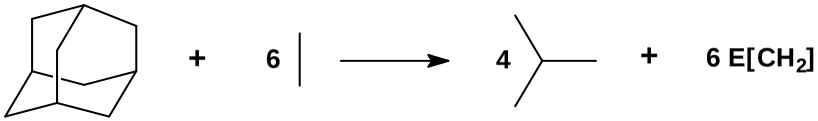	6.2	6.0[223], 6.48[227]
83	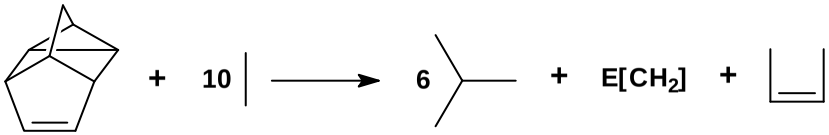	50.4	–
159	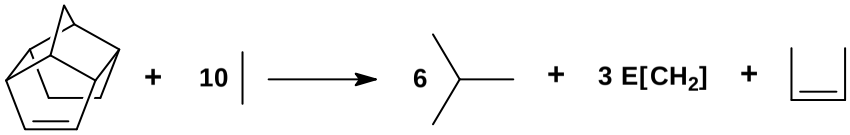	32.2	–
127	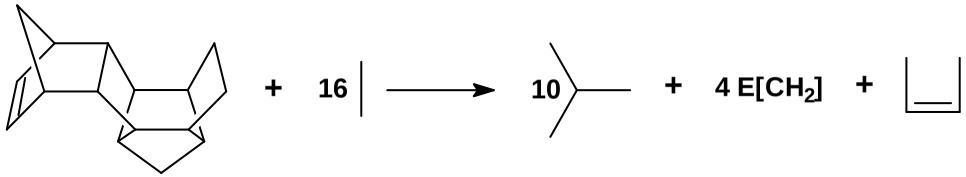	55.9	–
3	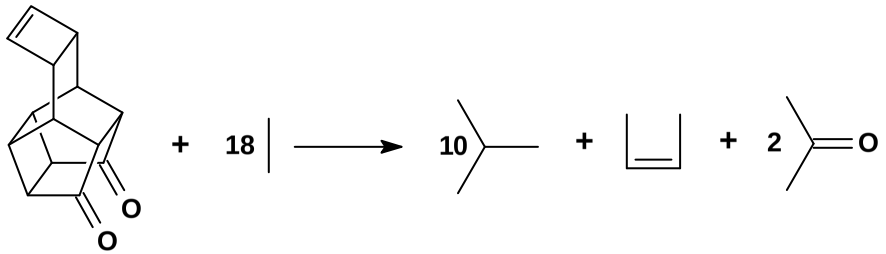	77.7	–

In this study, a method was developed to estimate the RSE released when only the cycloalkenyl fragment of a polycyclic compound is opened. The abbreviation RSE^f will be used to indicate this fraction of the total RSE. The most obvious approach to RSE^f is to use a homodesmotic reaction of the form given in **Scheme 3.3**.

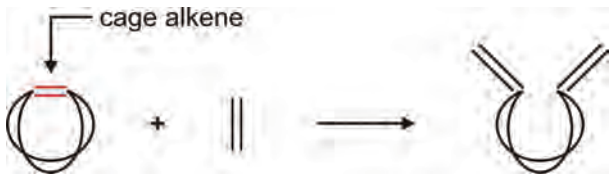

Scheme 3.3: Homodesmotic reaction used to calculate RSEs of cage alkenes.

To validate this approach, stepwise opening of the rings in norbornene was considered. This method entails opening of the first ring (RSE^f) followed by determination of the ring strain energy (RSE^r) of the remaining fragment (**Scheme 3.4**). It was found that the sum of the two ring opening steps agrees well with the total ring strain energy (RSE^{tot}) calculated for norbornene. The same method was applied to a number of systems and it was concluded that the total RSE is generally equal to the sum of RSE^f and RSE^r. Examples are reported in **Table 3.3**. This agreement is taken as support that the RSE energy obtained from the reaction in **Scheme 3.3** represents the part of the RSE that can be used as an indicator of ROMP reactivity.

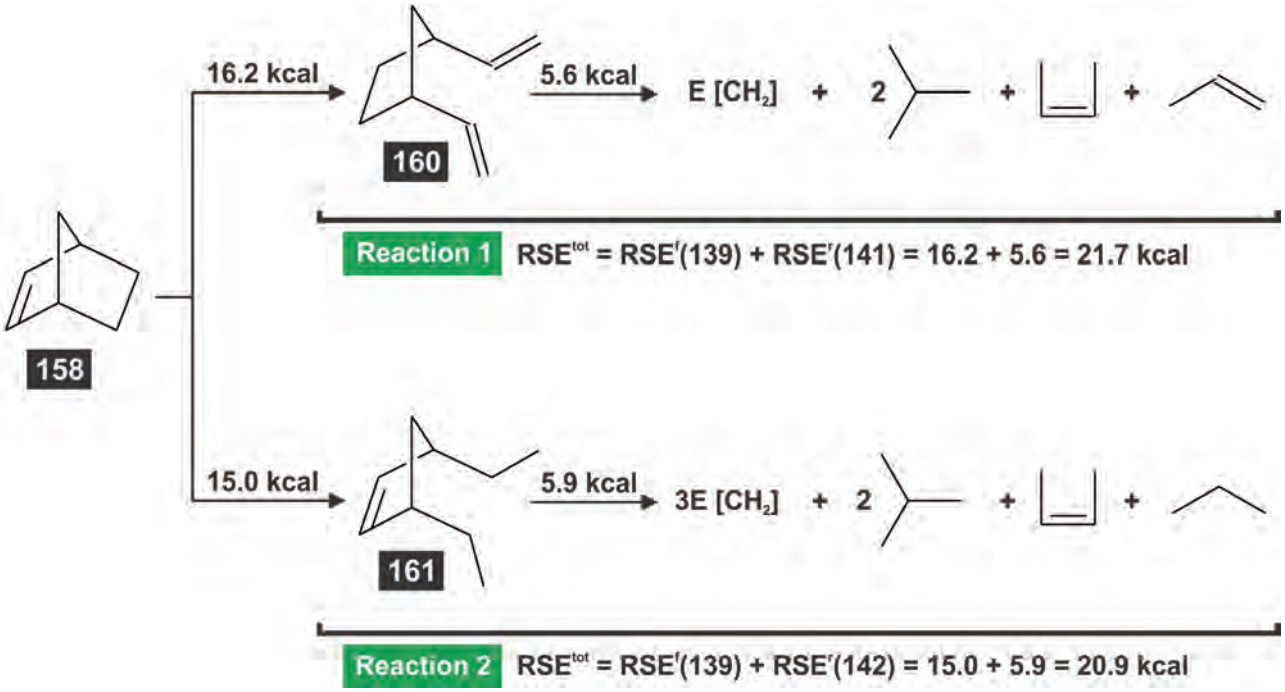

Scheme 3.4: Stepwise opening of the rings of norbornene.

Table 3.3: Total and fractional ring strain energies of selected monomers

Structure	RSE (kcal·mol^{-1})			
	RSE^{tot}	RSE^{f}	RSE^{r}	RSE^{f} + RSE^{r}
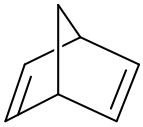 **162**	32.3	26.6	7.4	34.0
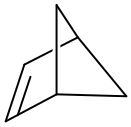 **163**	52.1	31.5	22.4	53.9
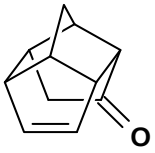 **1**	29.6	2.6	27.8	30.4

Hejl *et al*.[219] suggested that the ROMP of simple and substituted monocyclic alkenes should be possible if the RSE is more than 3.4 – 4.4 kcal·mol^{-1}. In this study, the applicability of this benchmark to cage alkenes was investigated. **Figure 3.5** shows the fractional ring strain of a number of cyclic alkenes.

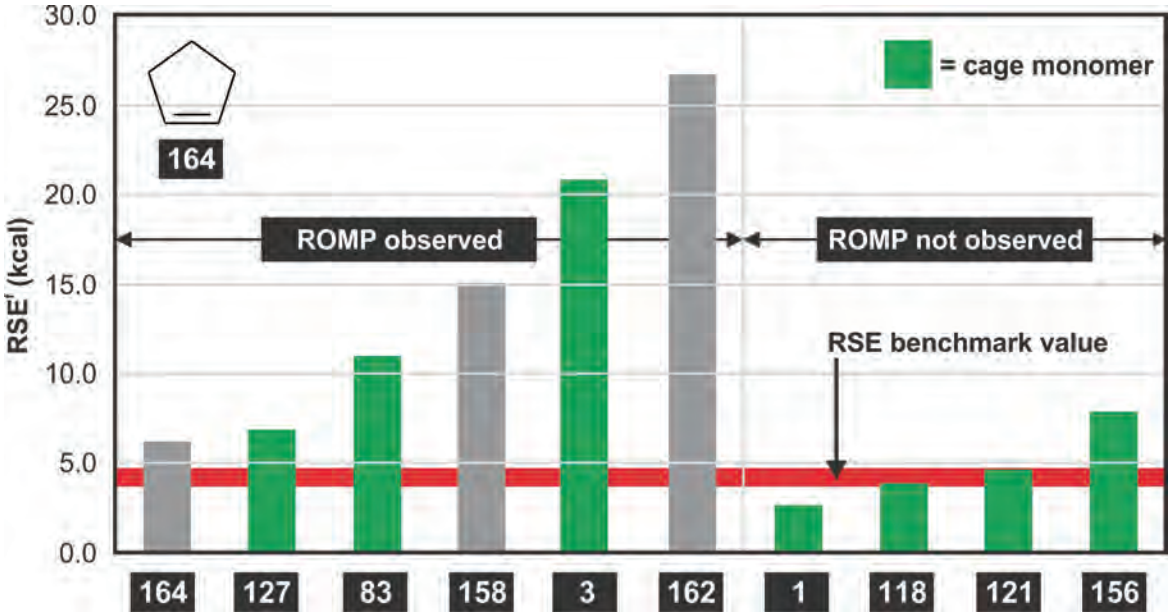

Figure 3.5: RSE^{f}s of various monomers.

The graph shows that the lack of reactivity of **1**, **118** and **121** could possibly be ascribed to low ring strain. The RSE^f value of **121** is difficult to interpret since the benchmark for ROMP of cage alkenes is not known exactly. The RSE^f value of **156** is even more problematic since this value should be sufficient to affect ROMP. It should be noted that the RSE^f of **156** is more than that of **127**, which did undergo ROMP to some extent. These facts may tip the scales in favour of an explanation that is not related to ring strain. It is clear from the interpretations of the graph in **Figure 3.5** that lack of ring strain is not the only factor influencing the reactivity of cage alkenes towards the Grubbs-I and Grubbs-II catalysts. Consideration of the results obtained for the cage alkene **127** suggests that the RSE^f required for successful ROMP of cage alkenes might be substantially higher than that required for ROMP of monocyclic alkenes. Higher RSE^f is probably required to compensate for the higher steric demand associated with the rigid and bulky nature of cage alkenes. **Figure 3.5** also shows the substantial influence of functional groups on the RSE^fs of cage alkenes. The RSE^fs calculated for **1**, **118**, **121** and **156** differ by 5.3 $kcal \cdot mol^{-1}$. In conclusion, it can be stated that low ring strain implies low reactivity towards ROMP, but that high ring strain does not necessarily mean high reactivity towards ROMP.

3.3.2. Energy profiles and the ROMP mechanism

The energy profiles for the ROMP of various monomers have been assembled from calculations with the DMol^3 application in Accelrys Materials Studio® 5.0 at the GGA-PW91/DNP level of theory. The steps shown on the energy profiles are based on the accepted mechanism for ROMP (➡ p. 10). **Figure 3.6** is a hypothetical energy profile that is provided to aid in the interpretation of the experimental energy profiles provided in this study.

The following steps can be distinguished on the energy profile:

- **Step 1:** A → B, Dissociation of PCy_3.
- **Step 2:** B → C, Association of the alkene functionality of the monomer.
- **Step 3:** C → D, Formation of the metallacyclobutane.
- **Step 4:** D → E, Fragmentation of the metallacyclobutane and formation of a new carbene.
- **Step 5:** E → F, Dissociation of the alkene functionality.

The catalytic cycle for ROMP consists of the repetition of **Step 2** – **Step 5**.

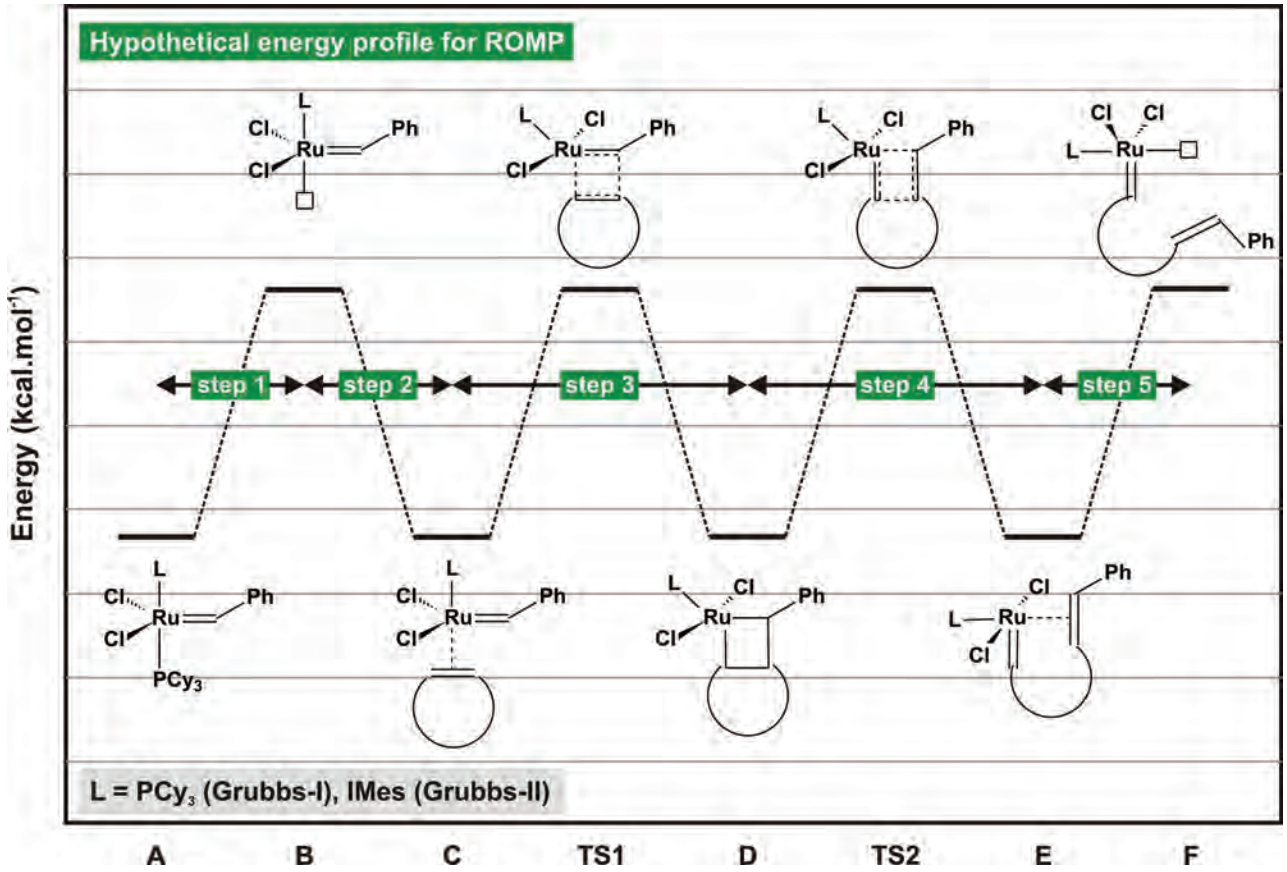

Figure 3.6: Hypothetical energy profile for ROMP.

3.3.2.1. Energy profiles for the ROMP of cage monomers

Two reference compounds from the literature were selected for use in this study (**Table 3.4**).

Table 3.4: Reference compounds

Monomer	Grubbs-I		Grubbs-II		ROMP
	Yield (%)	Reference	Yield (%)[1]	Reference	
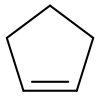 **164**	48 – 92	[219]	51 – 87	[219]	yes
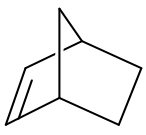 **158**	95 – 99	[92]	95 – 97	[95]	yes

[1] Variation in yield due to variation in initial monomer concentrations.

Norbornene (**158**) is extremely easy to polymerise by ROMP. Therefore, compounds such as cyclopentene (**164**) or 1,5-cyclooctadiene are used to test the ability of new catalysts to catalyse the ROMP reaction.[88] Comparisons between the energy profiles of these references and those of cage monomers can yield valuable information about the reactivity of the latter. **Figure 3.7** shows the calculated energy profiles for the reactions between the Grubbs-I catalyst and monomers **127**, **3**, **158**, **159**, and **164**.

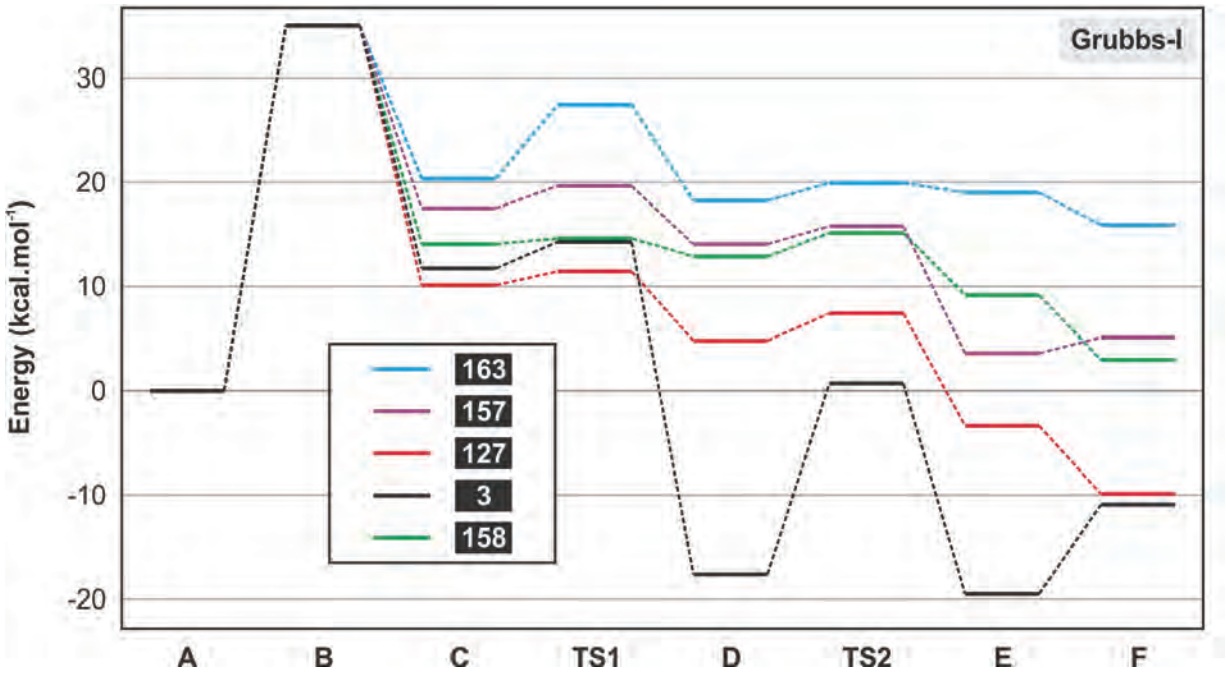

Figure 3.7: Energy profiles for the reaction of the Grubbs-I catalyst with various monomers.

Considering these energy profiles it appears that monomers **127** and **3** should be easier to polymerise by ROMP than monomer **164**. These predictions agree reasonably well with the experimental results. Both monomers **3** and **127** underwent ROMP although the reaction with **127** only produced 7% polymer. Similar results were obtained employing Grubbs-II in calculations. These energy profiles do not reveal any obvious reasons for the observed experimental results obtained with endocyclic monomers with a TCU framework.

Step 4 could be a crucial limiting step in the ROMP of endocyclic monomers with a TCU framework. This step leads to the formation of structure **D** (**Figure 3.6.**). Different monomers can be included into the metallacyclobutane fragment of structure **F** and different catalysts can be used. These different possibilities will be distinguished by using an abbreviation of the form **D-Gr^{x}-No** Here **Gr^{x}** represents Grubbs-I (Gr^{I}) or Grubbs-II (Gr^{II}) and **No** is the monomer number. For example, **D-Gr^{II}-121** refers to structure **D** formed by the association of monomer **121** with the Grubbs-II catalyst.

Figure 3.8 compares the geometry of **D-Gr^{II}-159** and **ethyl-D-Gr^{II}-83**. The most striking difference between these structures is the close proximity of the hydrogen atoms in **D-Gr^{II}-159**. Comparison of metallacyclobutane intermediates formed from different endocyclic TCU alkenes reveals that they all share this structural feature. A possible explanation for the observed experimental results is that TCU alkenes are unable to form metallacyclobutane intermediates during the ROMP reaction in the presence of Grubbs-I and Grubbs-II. This explanation is aligned with the results obtained from the NMR experiments with **1** described earlier (➡ p. 77).

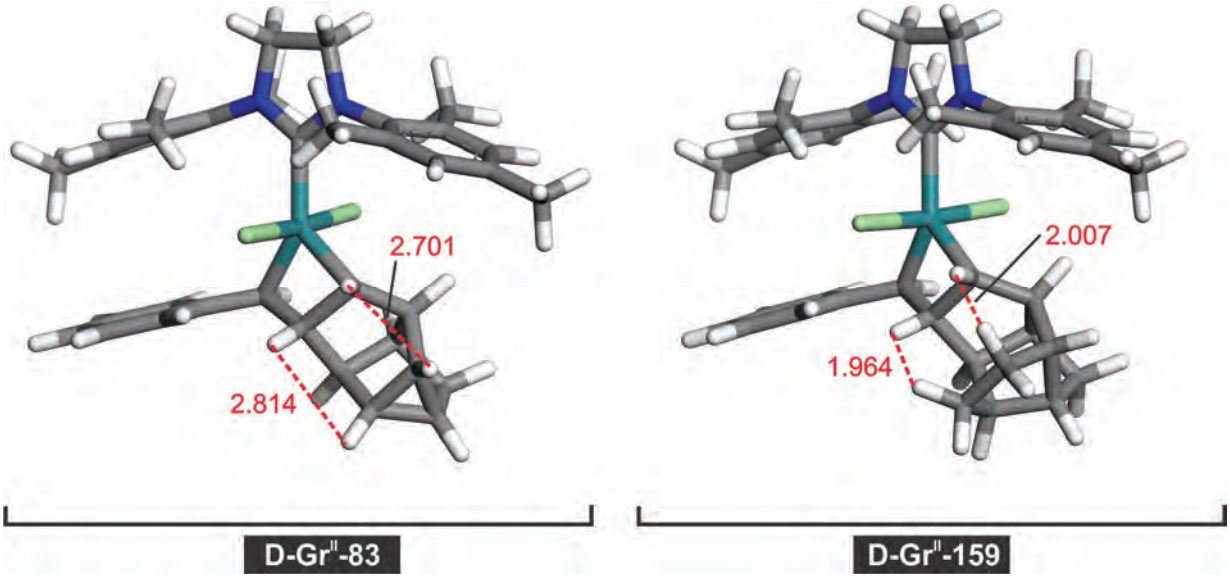

Figure 3.8: Comparison of the geometry of **D-Gr^{II}-159** and **D-Gr^{II}-83**.

Step 5 could also be an important limiting step during the ROMP of endocyclic cage monomers with a TCU framework. The fragment of the growing polymer ("polymer fragment") formed by the first monomer needs to dissociate in this step (**Figure 3.9**).

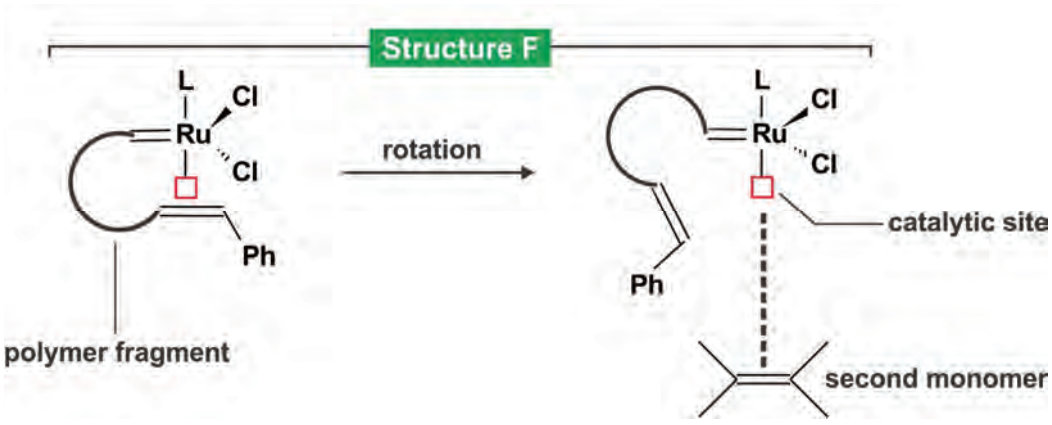

Figure 3.9: Importance of **Step 5** in the catalytic cycle.

This exposes the active site of the catalyst and enables a second monomer to associate with the catalyst. Inability of the polymer fragment to rotate and expose the catalytic site will inevitably lead to an unreactive ROMP system. **Step 5** yields structure **F**. Different monomers can be included into the polymer fragment of structure **F** and different catalysts can be used. These different possibilities will be distinguished by using an abbreviation of the form **F-Gr^{x}-No** as described previously.

Examinations of ball-and-stick models of structure **F** showed that the rigid nature of the TCU framework may prevent sufficient rotation to expose the catalytic site. The ball-and-stick models of structure **F** have the functional groups of the different endocyclic TCU monomers consistently pointing away from the catalytic site. The influence of functional groups on the availability of the catalytic site should therefore be minor. Molecular modelling with Materials Studio® did not give such clear results as the ball-and-stick models. Geometric optimisation (GGA-PW91/DNP) of structure **F** with Materials Studio® did not yield consistent results. The software appeared to keep the structure **F** uncomfortably close to that of the original drawing. As a result, further calculations were performed with Spartan® 10 (Hartree-Fock/3-61G). These calculations appeared to yield more satisfactory results.

Two orientations are possible when an endocyclic TCU alkene coordinates with structure **B** during **Step 2** of the ROMP mechanism. The resulting structures of **F** were geometrically optimised and compared. Both structures adopted a lowest energy configuration in which the active site was blocked. An example of this result is shown in **Figure 3.10**.

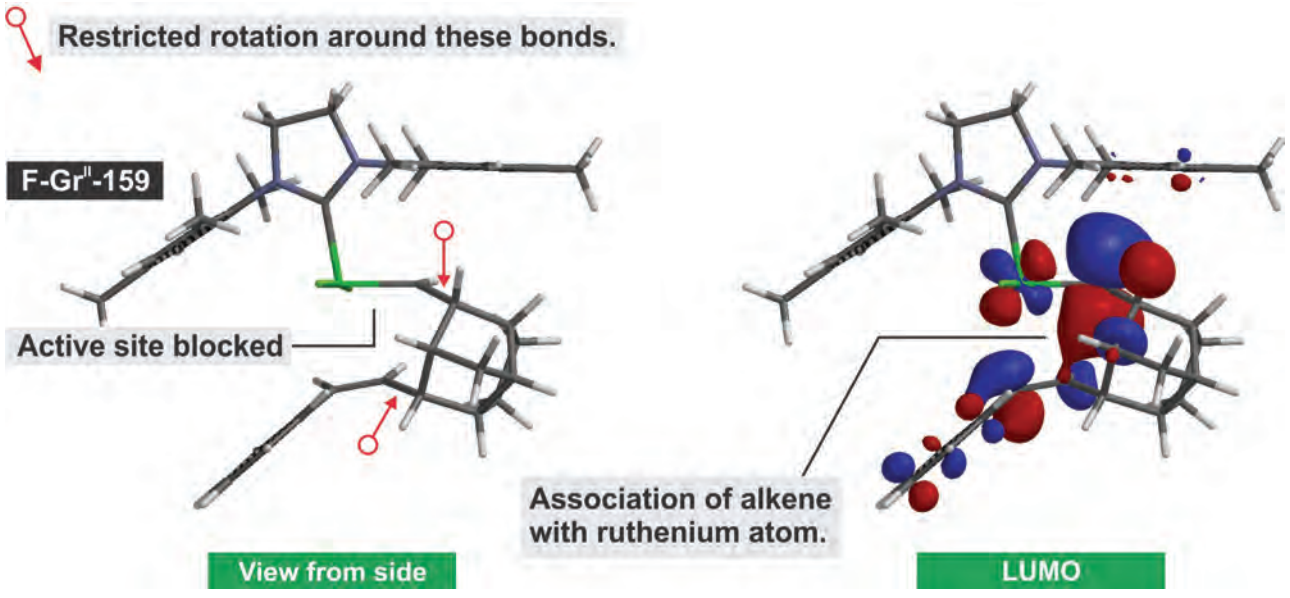

Figure 3.10: A possible structure of **F-Gr^{II}-159**.

The representation of the LUMO in **Figure 3.10** seems to indicate that the alkene functionality stays associated with the central ruthenium atom preventing exposure of the catalytic site and association of the second monomer. The situation can possibly explain the unreactive nature of endocyclic TCU alkenes towards Grubbs-I and Grubbs-II.

For reference purposes the structures of **F-Gr^{II}-3** and **F-Gr^{II}-158** were geometrically optimised (**Figure 3.11**). Structure **F-Gr^{II}-3** adopted a configuration similar to that of **F-Gr^{II}-159**. However, it appears that the alkene functionality is not as strongly associated with the central ruthenium atom and that the structure may be able to adopt a configuration in which the active site is exposed. Examination of a ball-and-stick model of **F-Gr^{II}-3** suggests that this structure has significant freedom of movement compared to **F-Gr^{II}-159**. In contrast to the cage alkenes, the lowest energy configuration of **F-Gr^{II}-158** is one in which the active site is exposed (**Figure 3.11**). In conclusion, it appears that cage alkenes generally adopt a configuration in which the active site is blocked and that exposure of the active site depends on the energy requirement.

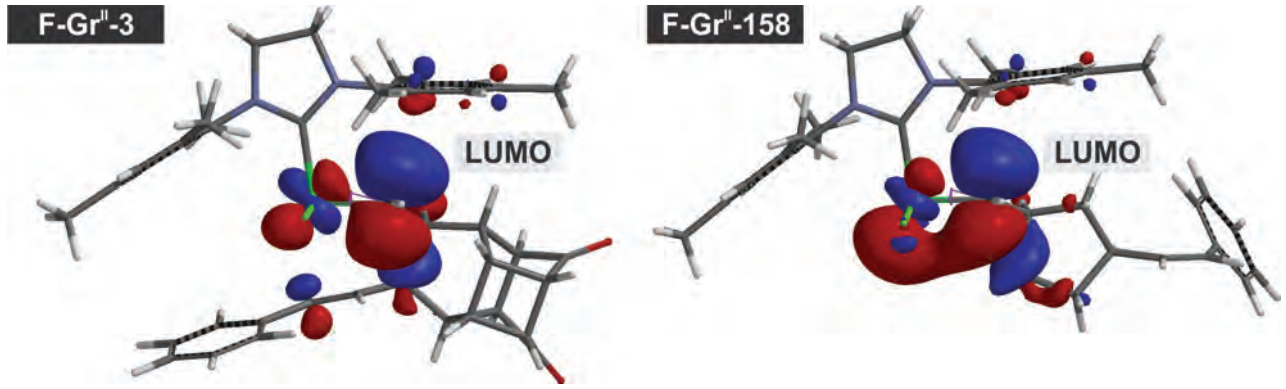

Figure 3.11: Possible structures of **F-Gr^{II}-3** and **F-Gr^{II}-158**.

It has been shown previously (➡ p. 84) that **1**, **118** and **121** suffer from low RSE^{f}s. It should be remembered that the RSE^f values of these three compounds are less than that of **127**, which underwent ROMP reactions to a small extent. However, the observed reactivity of these compounds may also be the result of steric problems incurred during the course of ROMP. The difficulty to interpret the RSE^f value of **156** has already been described. It seems that a blocked active site in **F-Gr^{II}-156** and/or the inability of the system to form **D-Gr^{II}-156** may be a more reasonable explanation for the inactivity of **156** towards ROMP. The calculated RSE^f value of **121** falls within the interval specified for the ROMP benchmark value. The lack of reactivity of **121** could therefore be due to low RSE^f and/or problems with structures **D-Gr^{II}-121** and/or **F-Gr^{II}-121**. In conclusion it seems that the lack of ROMP reactivity of endocyclic TCU alkenes may be ascribed to any combination of low RSE^f, inability to form structure **D** or formation of structure **F** in which the active site is blocked. In my opinion the importance of the steric effects outweighs that of RSE^f.

3.3.3. The effect of substituents on ROMP reactivity

The structure of the monomer used in ROMP influences both the properties of the polymer and the ease of polymerisation. It has been shown that substituents on norbornene influence the **rate** of ROMP (**Scheme 3.5**).[1] Catalyst **167** reportedly polymerises norbornene (**158**) about 4000 times faster than 2-norbornene-5-*t*-butylester (**165**) and >10^4 times faster than 2-norbornene-5,6-dimethyldiester (**166**). The marked difference in the rate of ROMP is not completely understood, but steric factors and complexation of the monomer with the catalyst may be involved.[1]

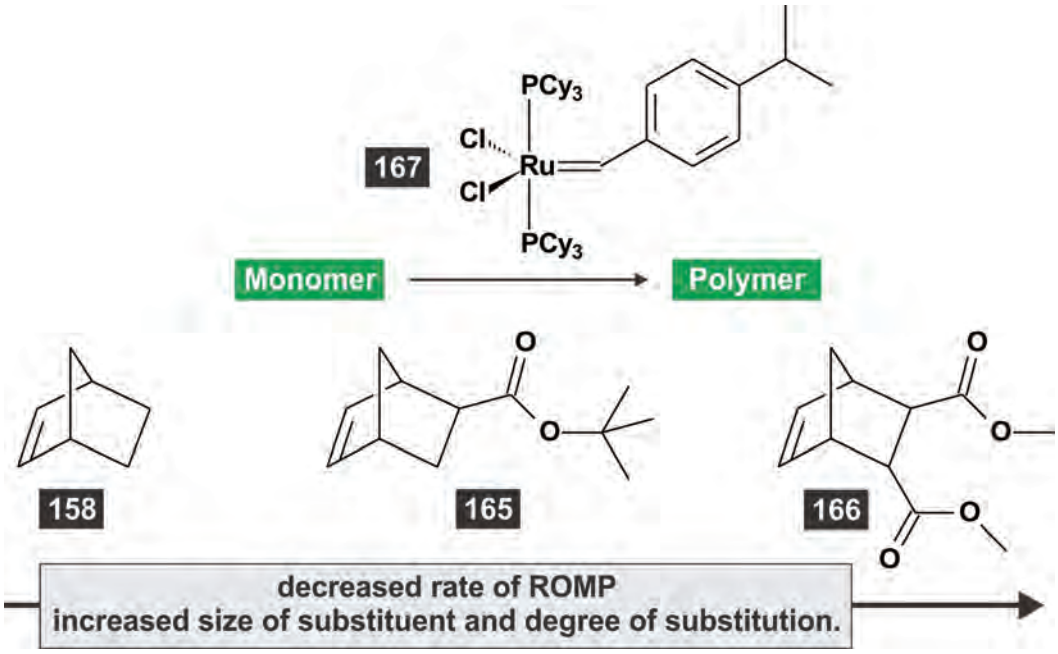

Scheme 3.5: Influence of substituents on the rate of ROMP.

In another example *anti*-7-methylnorbornene (**168b**) was shown to polymerise selectively from a mixture of *syn*- and *anti*-isomers (**Scheme 3.6**).[121,228]

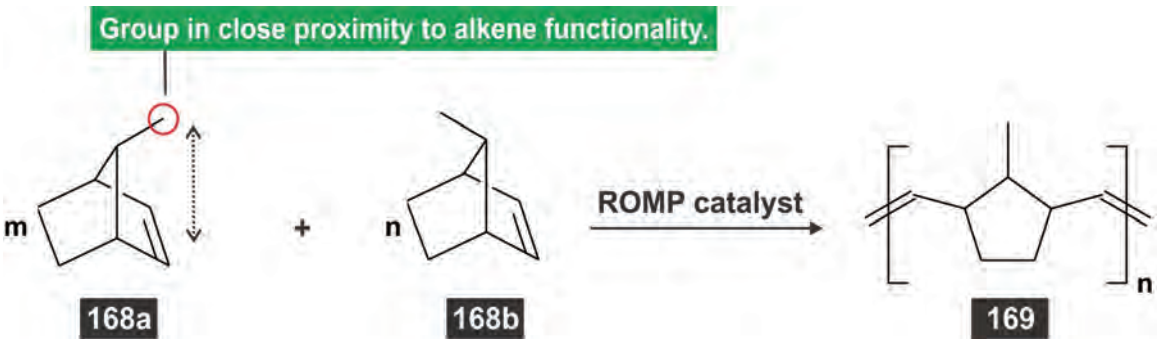

Scheme 3.6: ROMP of *syn*- and *anti*-isomers of 7-methylnorbornene.

The difficulty observed in attempts to ROMP *syn*-7-methylnorbornene (**168a**) is most probably a reflection of the methyl group being situated in close proximity to the alkene functionality. Similar influences may have a major effect on the reactivity of cage alkenes towards ROMP. Substituents in the 5-position and 6-position of the norbornene structure do not seem to have much influence on the **extent** of the ROMP reaction. **Table 3.5** shows some examples of norbornene derivatives with large substituents in the 5-position and 6-position that still took part successfully in the ROMP reaction with Grubbs catalysts.

Table 3.5: Influence of substituents on the ROMP reactions

Monomer	Catalyst	Yield (%)	Reference
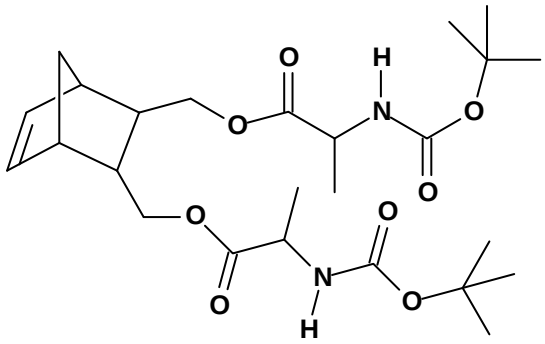 **170**	Grubbs-II	>98	[229]
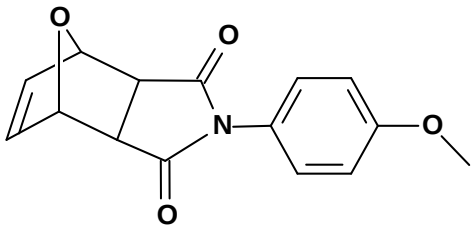 **171**	Grubbs-I	66	[230]
	Grubbs-II	88	
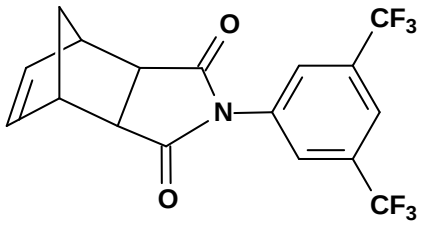 **172**	Grubbs-I	91 – 93	[231]
	Grubbs-II	94 – 98	
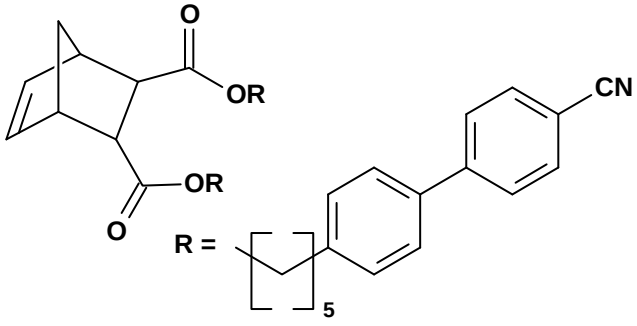 **173**	Grubbs-II	78	[232]

Experimental evidence suggests that substituents on the olefinic carbons atoms of cage alkenes may inhibit ROMP. Lautens *et al*.[119] reported that deltacyclene derivatives with a phenyl or butyl substituent on one of the olefinic carbon atoms did not undergo ROMP to an appreciable extent (**Scheme 3.7**).

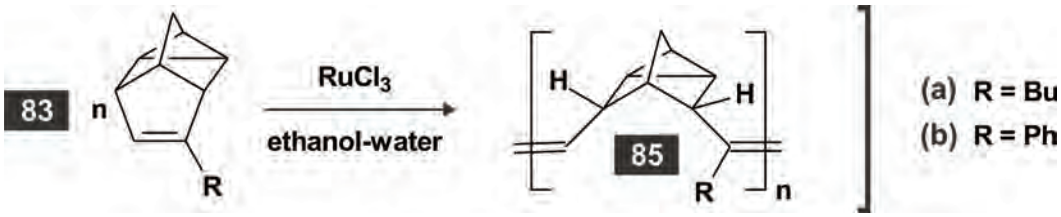

Scheme 3.7[119]**:** ROMP of substituted deltacyclene.

The cage alkenes used in this study are not more bulky than the monomers presented in **Table 3.5** (➡ p. 92) and do not have substituents on the olefinic carbon atoms. ROMP of these monomers thus seems more promising than indicated by the experimental results obtained thus far.

3.3.3.1. The effect of substituents on HOMO-LUMO interactions during ROMP

The association of the monomer to the catalyst during ROMP can be described in terms of favourable HOMO-LUMO overlap. A representative example is shown in **Figure 3.12**. The representation shows that frontier orbitals of suitable magnitude and orientation are available to describe the bonding between the ruthenium carbene **174** and cyclopentene (**164**).

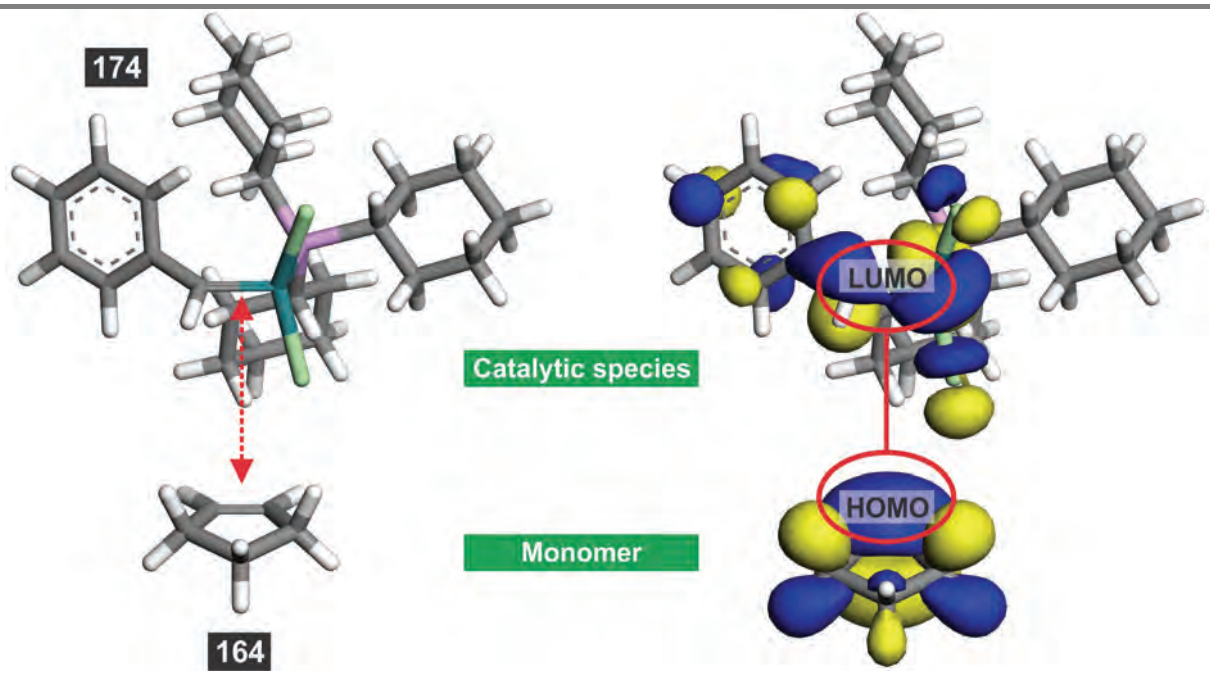

Figure 3.12: HOMO-LUMO interaction of norbornene and the active catalytic species.

Table 3.6 shows representations of the HOMO, NHOMO and total electron densities of the cage monomers used in this study as well as the simplified structures **159** and **175**. Examination of these models reveals that the cage alkenes **118**, **121**, and **156** do not have HOMOs or NHOMOs that protrude through their total electron densities. If there is a link between the reactivity of these cage alkenes and the relative sizes of the HOMOs and NHOMOs is uncertain. The cage alkene **3** shows significant ROMP reactivity even though it has small HOMO and NHOMO electron densities in the region of its alkene functionality. The simplified structures **159** and **175** have large HOMO electron densities in the regions of the alkene functionalities. It is also worthwhile to note that the RSE[f] of **159** is substantially higher than that of **1**. Synthesis of these monomers therefore seemed a worthwhile investment.

3.4. Potentially improved ROMP monomers

3.4.1. Preparation of potentially improved monomers

Decarbonylation of **1** and **3** yielded the cage alkenes **159** and **175**, respectively (**Scheme 3.8**). The NMR spectra of both compounds are simplified by symmetry.

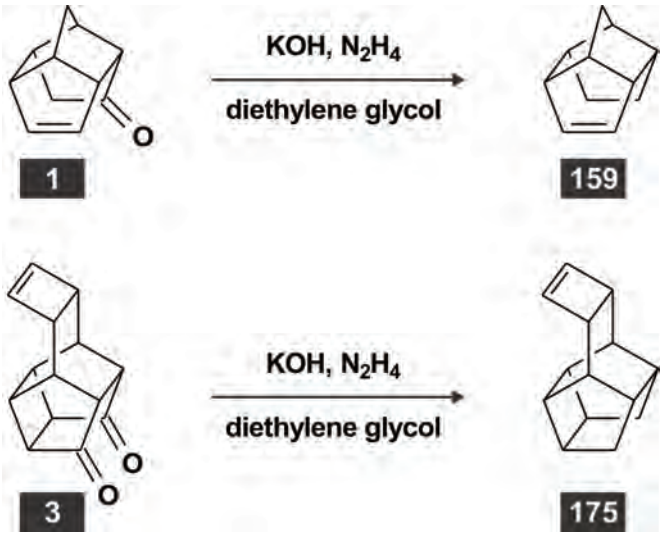

Scheme 3.8: Decarbonylation of cage ketones.

The 150 MHz ^{13}C NMR spectrum of tetracyclo[6.3.0.0^{4,11}.0^{5,9}]undec-2-ene (**159**) shows seven signals that can be associated with seven non-equivalent carbon atoms. The signal at δ_c 138.8 represents the two olefinic carbon atoms. The DEPT-135 spectrum indicates the presence of two methylene groups at δ_C 28.3 and δ_C 31.2. The signal at 1.52 ppm in the 600 MHz ^1H NMR spectrum of **159** was assigned to the methylene protons at C-10. The methylene protons at C-7 register at δ_H 1.48 (H-7$_a$) and δ_H 1.60 (H-7$_s$). The assignments of the remaining signals in the ^1H NMR and ^{13}C NMR spectra followed from COSY and HSQC data (**Table 3.7**).

TABLE 3.6: HOMO, NHOMO and total electron density of cage alkenes tested in this study

Substrate		HOMO	NHOMO	HOMO superimposed on total electron density	NHOMO superimposed on total electron density
1		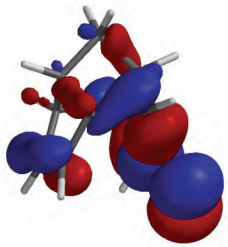	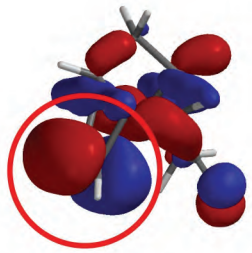	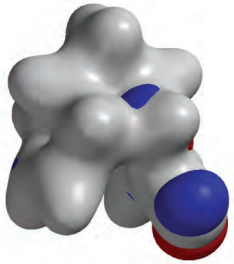	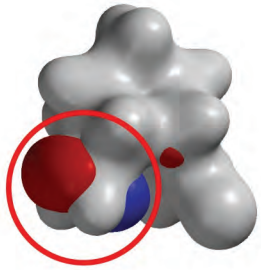
118		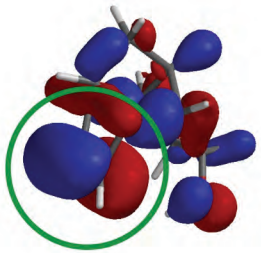	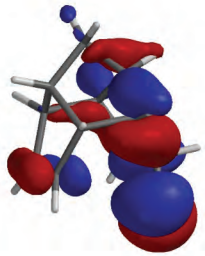	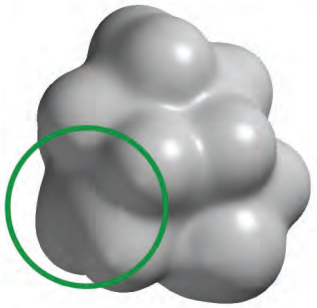	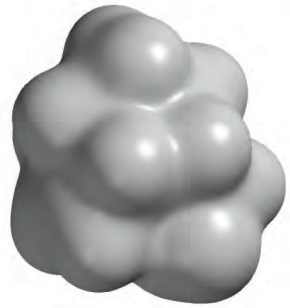
121	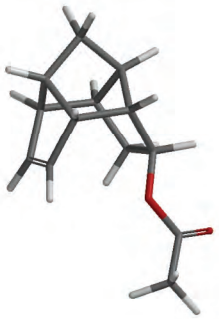	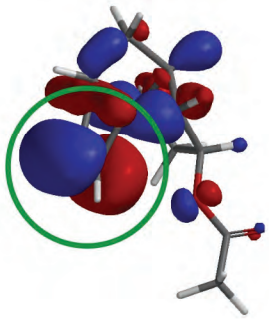	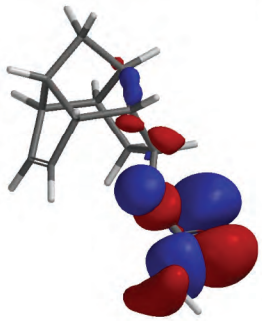	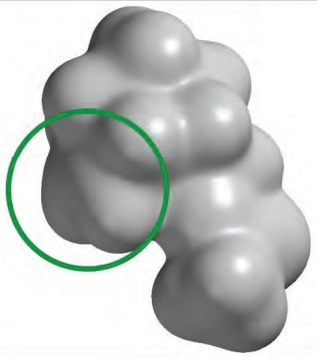	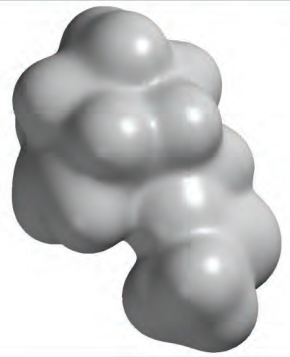

TABLE 3.6: HOMO, NHOMO and total electron density of cage alkenes tested in this study (Continued)

	Substrate	HOMO	NHOMO	HOMO superimposed on total electron density	NHOMO superimposed on total electron density
156	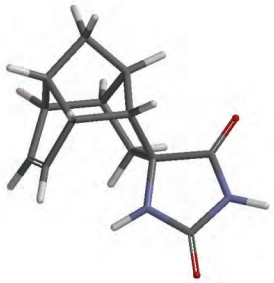	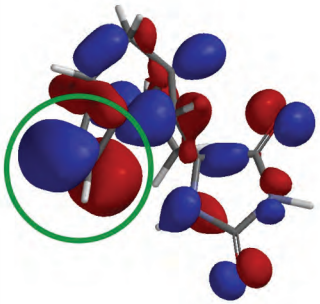	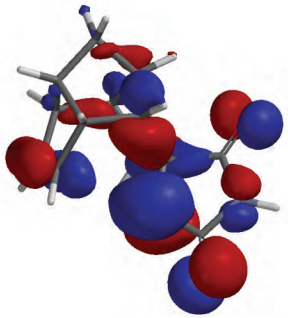	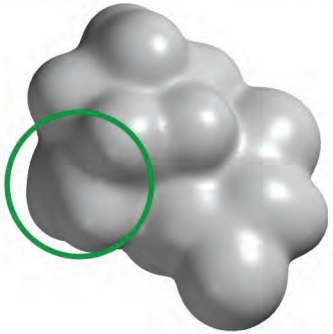	
127	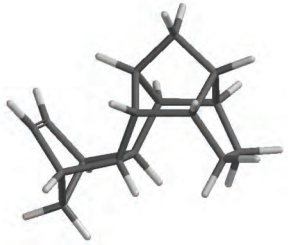	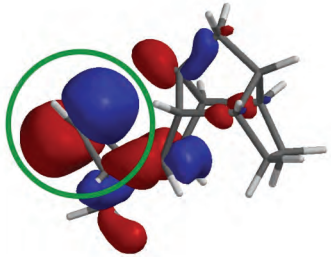	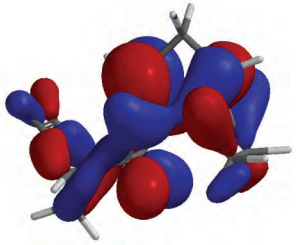	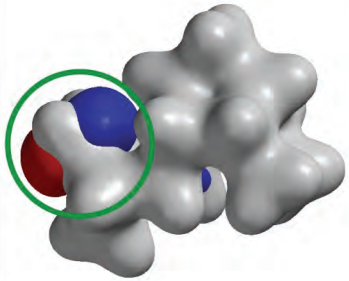	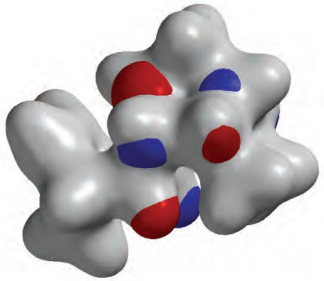
159	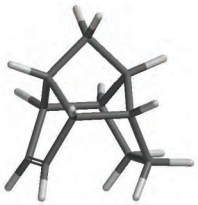	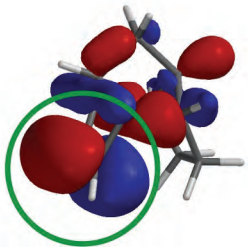	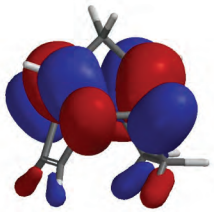	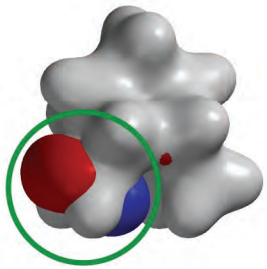	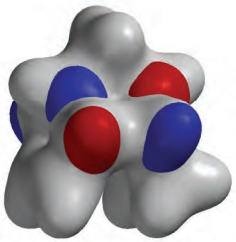

TABLE 3.6: HOMO, NHOMO and total electron density of cage alkenes tested in this study (Continued)

Substrate		HOMO	NHOMO	HOMO superimposed on total electron density	NHOMO superimposed on total electron density
3	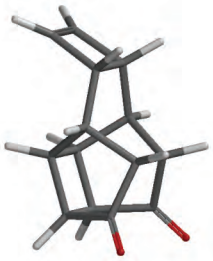	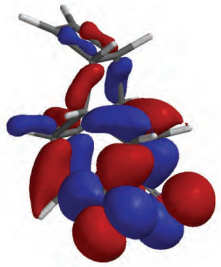	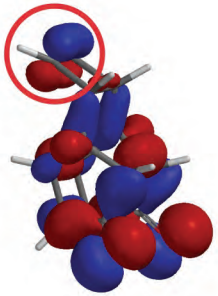		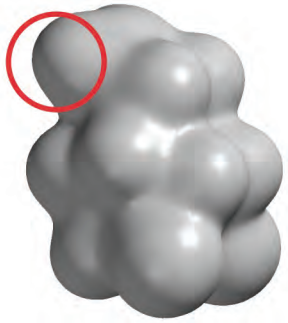
175	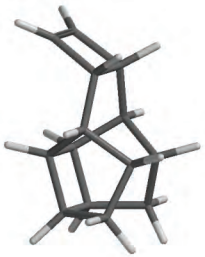	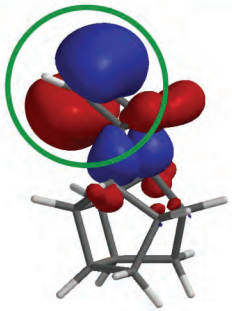	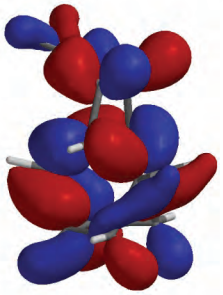	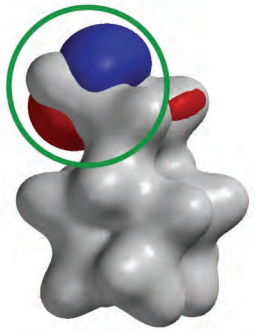	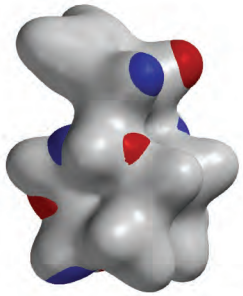

Table 3.7 ^{1}H and ^{13}C NMR data^{x} of 159

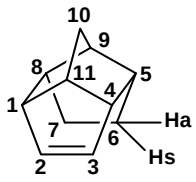

159

Number C/H	δ^{y}_{H} (ppm)	J (Hz)	δ^{y}_{C} (ppm)
1/4	2.38	-	47.6
2/3	6.06	-	138.8
5/8	2.17	-	46.2
$6_a/7_a$	1.48	7.9	28.3
$6_s/7_s$	1.60	- [z]	
9	2.38	-	52.7
10	1.52	-	31.2
11	2.75	-	57.8

[x] ^{1}H NMR spectrum: 600 MHz, ^{13}C NMR spectrum: 150 MHz

[y] Solvent: $CDCl_3$

[z] Coupling constant could not be determined due to overlap of these proton signals.

The 150 MHz ^{13}C NMR spectrum of hexacyclo[8.4.0.0^{2,9}.0^{3,13}.0^{4,7}.0^{4,12}]tetradec-5-ene (**175**) exhibits seven signals that can be associated with seven non-equivalent carbon atoms. The signal at δ_c 140.5 represents the two olefinic carbon atoms. The DEPT-135 spectrum indicates the presence of a single methylene group at δ_C 27.1 ppm. Through the HSQC spectrum this signal can be linked to the signals resonating at δ_H 0.86 and δ_H 1.78 in the ^{1}H NMR spectrum. Therefore these signals were assigned to H-11$_a$/H-14$_a$ and H-11$_s$/H-14$_s$, respectively. The assignments of the remaining methine signals in the ^{1}H NMR and ^{13}C NMR spectra are based on COSY and HSQC experiments (**Table 3.8**).

Table 3.8 ^{1}H and ^{13}C NMR data^{x} of 175

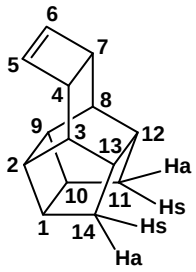

175

Number C/H	δ^{y}_{H} (ppm)	J (Hz)	δ^{y}_{C} (ppm)
1/10	2.63	-	36.7
2/9	2.50	-	36.1
3/8	1.51	-	41.1
4/7	2.94	-	41.0
5/6	6.16	-	140.5
12/13	2.18	-	37.3
$11_a/14_a$	0.86	11.7	27.1
$11_s/14_s$	1.78	11.7	

[x] ^{1}H NMR spectrum: 600 MHz, ^{13}C NMR spectrum: 150 MHz

[y] Solvent: $CDCl_3$

3.4.2. ROMP of potentially improved monomers

The new monomers **159** and **175** were tested for ROMP reactivity. The results of these tests are shown in **Table 3.9**. Monomer **175** reacted with both Grubbs-I and Grubbs-II. Yields were between 73 and 84%. Monomer **159** was not reactive towards ROMP under the same reaction conditions.

Table 3.9: ROMP of new cage monomers with Grubbs-I and Grubbs-II

Monomer	Solvent	Catalyst	Mon :cat	Time (h)	t (^{o}C)	Yield
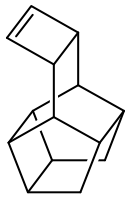 **175**	THF	Grubbs-I	50:1	12	25^{o}C	73%
	THF	Grubbs-II	50:1	12	25^{o}C	83%
 **159**	THF	Grubbs-I	50:1	24	25^{o}C	–
	THF	Grubbs-II	50:1	24	25^{o}C	–

The experimental results obtained for **159** were investigated further with NMR spectroscopy. A reaction mixture consisting of **159** and Grubbs-II in CDCl3 was monitored for three hours at 40^{o}C. NMR data were collected at 10-minute intervals. Information about the NMR experiment is provided in **Table 4.2** (➡ p. 121). The progress of the possible ROMP reaction was determined from the ratio of the integral of the olefinic protons at δ_H 6.06 and the TMS signal at δ_H 0.00. Some result of the NMR experiment is reported in the spectral data section (➡ p. 173 - 174). The outcome of the experiment was the same as that obtained previously for the reaction mixture of **1** and Grubbs-II. No precipitate formed during the monitoring process and no polymer product could be detected in the NMR spectra. These results indicate that the cage monomer **159** is not reactive towards ROMP and does not coordinate with the catalyst. Extrapolation of this conclusion to all endocyclic alkenes with a TCU framework seems in order.

3.5. Conclusion

The calculated RSE^f of a cage alkene is a useful quantity that can be used as a first indication of ROMP reactivity. **Table 3.10** is a list of the monomers used in this study. Considering this information only, a threshold RSE^f can be estimated at about 7 kcal·mol^{-1}. However, RSE^f cannot be considered in isolation since endocyclic TCU alkenes may very likely suffers steric problems during the ROMP process. For example, considering only the RSE^f of **156** will lead to an incorrect conclusion. It was also pointed out earlier that the position of the functional groups in the endocyclic TCU alkenes considered in this study should not interfere when the monomer associates with the catalyst or during subsequent steps. It is therefore likely that the ROMP reactivities of endocyclic TCU alkenes are independent of RSE^f.

Table 3.10: Possible link between RSE^f and ROMP yield

Structure		RSE^f (kcal·mol^{-1})	Yield (%)
1	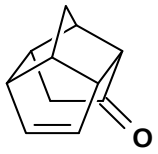	2.6	ROMP not observed
118	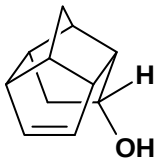	3.8	ROMP not observed.
121	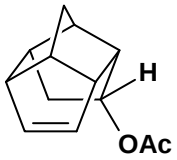	4.5	ROMP not observed.
159		5.9	ROMP not observed.
127	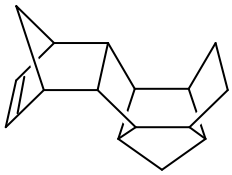	6.8	Grubbs-I: 7 Grubbs-II: 15
156	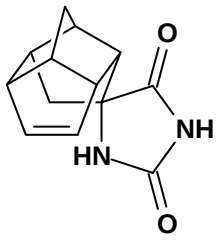	7.9	ROMP not observed.
3	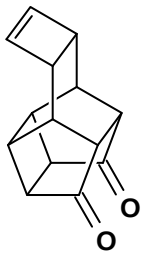	20.8	Grubbs-I: 21 Grubbs-II: 48
175	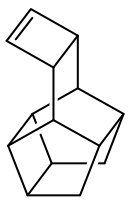	22.2	Grubbs-I: 73 Grubbs-II: 83

Energy profiles (➡ p. 87) were found to be an average predictor of ROMP reactivity in this study. The energy profile predicted that cage monomers **3** and **127** would undergo ROMP. However, some reactions that seemed probable based on their energy profiles were not observed experimentally. An example is the ROMP reaction of compound **159**. It is likely that steric effects are not represented sufficiently in the energy profiles. Consideration of the HOMO-LUMO interaction between the monomers and catalysts hinted at the improved ROMP reactivity of the decarbonylated compound **175**. However, FMO theory could not explain or predict the reactivity of **159** and the endocyclic TCU alkenes towards ROMP.

Any model regarding the reactivity of cage monomers should focus on the catalytic system and not on monomer structure only. A safe strategy to predict the ROMP reactivity of cage monomers seems to consider the integrated picture provided by combining the results of calculated RSE^fs, energy profiles, steric considerations and frontier orbitals. Cage alkenes that successfully underwent ROMP in this study exhibited the properties set out in the criteria given below. Those that were unsuccessful had one or more properties that could not be aligned with these guidelines.

The criteria for successful ROMP of cage monomers can be summarised as follows:

1. Sufficient fractional ring strain (RSE^f).
2. A reasonable energy profile when compared to a reference compound such as cyclopentene.
3. Ability to form a metallacyclobutane intermediate with reasonable distances between different parts of the cage fragment.
4. Sufficient ability of the polymer fragment to take on a conformation that exposes the catalytic site.
5. Sufficient size, shape and energy of HOMO and/or NHOMO at the alkene functionality of the cage monomer and of the LUMO at the catalytic site.

Criteria 3 – 4 can be reinterpreted for this study to mean that the monomer should not be an endocyclic alkene with a TCU framework.